

# INDOOR MAPPING USING MIMO RADIO CHANNEL MEASUREMENTS

Hassan Naseri      Jussi Salmi      Visa Koivunen

Aalto University, School of Electrical Engineering, Finland ({firstname.lastname}@aalto.fi)

Geometrical maps of the indoor environment are vital to many applications such as indoor localization and robot navigation. In this paper, a method for three-dimensional indoor mapping using multipath delay and direction estimates is developed. Required high-resolution estimates of multipath propagation path parameters are obtained using radio frequency measurements between two antenna arrays at multiple locations. A ray-tracing algorithm is developed for detecting specular propagation paths of radio signals and corresponding reflection points. A novel method is proposed to extract walls and other planar structures from the cloud of reflection points. The empirical results show an improved precision and enhanced geometric information compared to previous experiments.

**Index Terms**— Radar Imaging, SLAM, Multipath Exploitation

## 1. INTRODUCTION

Geometrical models and maps of the indoor environment are essential part of many applications and services, such as indoor localization, robot navigation, and first responders in emergency services. Multipath propagation of radio signals can be exploited to create such a map [1]. In this paper, we address the problem of estimating the location of a moving beacon and creating a three dimensional (3D) map of an indoor environment, given delay and angle estimates corresponding to multipath propagation paths. Such estimates may be acquired using microwave-frequency multiple-input multiple-output (MIMO) channel sounding measurements [3, 4].

Recently, there has been a growing interest in indoor mapping using radio-frequency or acoustic measurements. Results for ultra wide band (UWB) through-the-wall synthetic aperture radar (SAR) were presented in [5–11]. Multipath exploitation radar (MER) solutions for indoor environment were proposed in [12–14]. MER techniques mostly focus on point targets rather than extended targets and indoor mapping. Algorithms for estimating room geometry using range-only radio measurements have been proposed in [1, 15–17]. These techniques are applied to simple room geometries. Mapping techniques using acoustic delay measurements were presented in [18–20]. A combinatorial search method is proposed to assign received echoes to reflectors. Multipath-exploiting range-based simultaneous localization and mapping (SLAM) techniques have been proposed in [21–24]. These methods either produce a map of a sparse scene, i.e., few point targets, or a simple room geometry. A technique based on geometrical modeling was proposed in [25], which finds the geometry of large outdoor features. A closely related work was presented in [26, 27], where a ray-tracing method was used to detect scatterers corresponding to specular paths in an indoor environment. A recent work on the clustering of scattering points was proposed in [28].

In this paper, a novel algorithm is proposed for estimating the geometrical map of scattering environment using the estimated parameters of multipath propagation paths. The algorithm uses line-of-sight (LOS) paths for localization of a moving transmitter, and

single-bounce reflection (SBR) paths for finding reflection points. An SBR path is a ray between two nodes that is bounced from a reflector once, i.e., it is a first-order reflection. The proposed technique can be used for indoor mapping with measurements obtained by mobile wireless devices, provided that the resolution of angle and range estimates are sufficient. The algorithm is developed for the general case of having 3D angle estimates, which requires 2D or 3D antenna arrays. However, the technique can be adopted to the common case of uniform linear arrays. The original contributions of this paper are as follows.

1. A simple and reliable 3D ray-tracing technique is developed for detecting SBR paths and corresponding reflection points.
2. A novel method stemming from Hough transform [29] is specifically developed to detect SBR points in 3D measurements. This method finds walls and other planar reflectors.
3. Real-world measured data are used to evaluate the algorithm. A two dimensional (2D) floor map of the indoor environment is produced with higher precision and enhanced geometric information compared to [27]. To the best of authors' knowledge, there is no existing method that can find long segments of the walls and produce a map of a complex indoor environment using a similar signal bandwidth. The results are comparable to UWB SAR images that require a higher bandwidth and a more complex hardware [5].

The rest of this paper is organized as follows. Section 2 described the measurement model. The proposed localization and mapping algorithms are described in Section 3. Simulation results are presented in Section 4. Finally, Section 5 concludes the paper.

## 2. MEASUREMENT MODEL

A multipath radio channel can be modeled as a superposition of specular (concentrated) propagation paths plus a dense scattering component. Fig. 1 shows the double-directional multipath channel model for specular paths. The term “double-directional” refers to the fact that the channel is characterized by directional properties at both ends of the radio link. The model allows to exclude the characteristics of the measurement antennas from the channel at both ends.

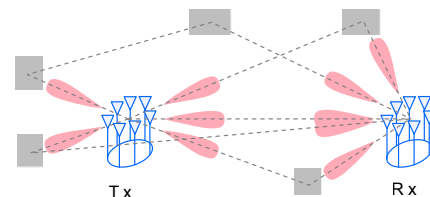


Fig. 1: Double directional structure of deterministic paths in a multipath radio channel. Both Tx and Rx have antenna arrays. Specular paths are reflected at scatterers (gray rectangles).

In MIMO channel sounding, a multipath radio channel is excited by a wideband test signal using transmit and receive antenna arrays at multiple locations [4, 30], e.g., with a moving transmitter array. The parameters of the double-directional channel model are estimated from the measurements. The parameters of a specular path in the double-directional channel model are direction-of-departure (DOD), direction-of-arrival (DOA), time-of-arrival (TOA), four polarimetric complex path weights, and Doppler frequency. DOD and DOA are (azimuth, elevation) angles at transmitter and receiver arrays respectively. The parameters are estimated using high-resolution estimation techniques [2]. Each propagation path is detected and initialized using a maximum likelihood (ML) technique. Then a state-space model is used to track the path parameters as the transmitter moves [3]. The algorithm also provides information about the variances of the parameters. In this work, the estimated parameters of the specular paths from [3, 31] are used to estimate the transmitter location and extract a scattering map of the environment. The whole procedure may be outlined as

$$\hat{\mathbf{H}} \rightarrow \hat{\boldsymbol{\theta}} \rightarrow \hat{\mathbf{P}} \rightarrow \hat{\mathbf{M}}, \quad (1)$$

where  $\hat{\mathbf{H}}$  is the estimated channel response in frequency domain;  $\hat{\boldsymbol{\theta}}$  is the estimated spatial and temporal parameters of the propagation paths,  $\hat{\mathbf{P}}$  is the location estimates of the actual and virtual transmitter-receiver pairs, and  $\hat{\mathbf{M}}$  is the scattering map of the environment. A virtual Tx is the source of a propagation path from receiver's point of view, if the path was a straight line. Similarly, a virtual Rx is the end of a path from transmitter's point of view. For an LOS path, virtual Tx and Rx are coinciding with physical Tx and Rx. For an SBR path, a virtual Tx (or Rx) is an image of the physical Tx (or Rx) at a reflector plane, see Fig. 2. A scattering map is a geometrical map (image) of the objects in the environment that reflect the measurement signal. The focus of this paper is on estimating  $\hat{\mathbf{P}}$  and  $\hat{\mathbf{M}}$ .

### 3. PROPOSED ALGORITHM

The proposed localization and mapping algorithm is described in this section. Table 1 summarizes the algorithm. Stage 1 in Table 1 is performed according to [31]. Stages 2 is a localization method developed in this work to estimate the trajectory of the transmitter. Stage 3 is a novel ray-tracing method to detect SBR paths and calculate corresponding reflection points. Stage 4 is a novel filtration and detection method stemming from Hough transform [29]. It finds the reflector planes corresponding to SBR paths and creates the final scattering map.

**Table 1** Summary of the algorithm stages

- |   |
|---|
| 1: Estimate specular propagation path parameters from MIMO channel measurements, see [31] for details.                                  |
| 2: Detect LOS path in each snapshot. Estimate and track Tx position. Calculate virtual Rx/Tx positions. See Subsection 3.1 for details. |
| 3: Detect SBR paths and find corresponding reflection points, see Subsection 3.2 for details.   |
| 4: Apply Hough detector to the scatter map to find reflector planes and create the final map, see Subsection 3.3 for details.           |

#### 3.1. Detecting LOS path and Localization

First, the power of each path is calculated as the sum of the squared polarimetric path weights. The path powers are compensated for

free-space path loss. The LOS path parameters are calculated as a weighted sum of the parameters from the shortest path and the strongest path in each snapshot. The weights are path powers. The position of the transmitter at each measurement point is given by the range and DOA of the LOS path. The orientation of the Tx is calculated using the DOD of the LOS path. The location and orientation of the receiver are used to build a frame of reference. The estimated Tx positions and orientations along each route are filtered to suppress error and remove outliers. The filter is a robust local regression method using iteratively re-weighted linear least squares (IRLS). A linear model assumes a constant speed for the transmitter in short intervals, i.e., in the span of the filter. The outliers are removed by iteratively re-weighting the points within the filter span. A bisquare weighting function gives smaller weights to the points farther from the center. This method, called "rlowess", is a part of the Curve Fitting Toolbox in MATLAB, see [32, chap. 6] for more details. By projecting parameters of all paths (not only LOS path) into the reference Cartesian coordinate system, we obtain locations of virtual transmitters and virtual receivers. Similar to LOS parameters, a robust smoothing filter is applied to virtual Rx and Tx positions. These virtual locations will be used for ray tracing to construct a scattering map.

#### 3.2. Detecting SBR paths and Scattering Points

In this work, only SBR paths are used to create an scattering map. SBR paths are detected using virtual Tx/Rx locations of each path other than the LOS. For each specular path, the line from Rx to virtual Tx and the line from Tx to virtual Rx are illustrated in Fig. 2. Since these

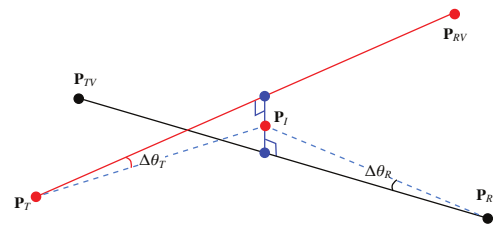


**Fig. 2:** Finding the reflection point for an SBR path.  $P_T$  and  $P_{TV}$  are actual and virtual Tx positions.  $P_R$  and  $P_{RV}$  are actual and virtual Rx positions. Due to errors, the estimated transmit and receive angles of an SBR path do not exactly match. The intersection point  $P_I$  is found where two rays are closest to each other.

two lines may not intersect in 3D space, least-Squares is used to find the closest points on two lines. The *intersection point* is found on the line between these two points, such that the angle differences from Tx and Rx paths are same, i.e.,  $\Delta\theta_R = \Delta\theta_T$  in Fig. 2. This angle is referred to as *intersection angle*. A path is detected as an SBR path if the following conditions are met:

- The *intersection angle* is smaller than a given threshold, which is two times the standard deviation of angle estimates.
- The length of the resulting SBR path is sufficiently close to the estimated path length.

There is a risk of spurious detection due to reflections from Tx/Rx bodies and nearby objects, e.g., the platforms on which the arrays are mounted. Hence, a path is discarded if (i) it is very close to the LOS path, (ii) the reflection point is very close to the transmitter or receiver, or (iii) the intersection point is outside the area of interest. To produce a scatter map of the environment, all detected SBR points are added to a 3D accumulator grid. This is done by producing a

weighted 3D histogram using path powers as weights. 2D images may be produced by slicing the 3D map.

### 3.3. Hough Detector for Extracting Reflector Planes

A 3D image processing algorithm is developed to enhance planar structures in the scatter map. The method is based on Hough transform [29]. Table 1 summarizes the proposed Hough detector method.

**Table 2** Summary of the Hough Detector stages

- |  |
|--|
| 1: Find reflector planes for SBR paths, transform to Hough space.  |
| 2: Create a 2D Hough image for walls and apply a smoothing filter.   |
| 3: Detect peak regions in the Hough image and find their centroids.  |
| 4: Transfer the detected peak regions to Cartesian coordinates and apply a directional smoothing filter to each cluster. |

First, a reflector plane is calculated for each SBR point. These planes are transformed to 3D Hough domain  $(\theta, \phi, \rho)$  and filtered, where  $\rho$  is the distance of the plane to the origin,  $\theta$  is the angle between the plane and xy-plane, and  $\phi$  is the angle between the plane and z-axis. It is assumed that an SBR path is a specular reflection where incident, normal, and reflected directions are coplanar. That is, they lie on a single plane, referred to as *path plane*, given by tree points: Tx, Rx, and reflection point. It is also assumed that an SBR path is reflected from a smooth flat surface, referred to as a *reflector plane*. The paths coming from non-flat surfaces will be filtered out after transformation to Hough domain. The locus of a *reflection point* for an SBR path is an ellipse lying on the path plane with foci at node positions and major axis equal to the path length. A reflector plane is perpendicular to the corresponding path plane; and is tangent to the corresponding SBR path ellipse [33], see Figure 3. Such a plane

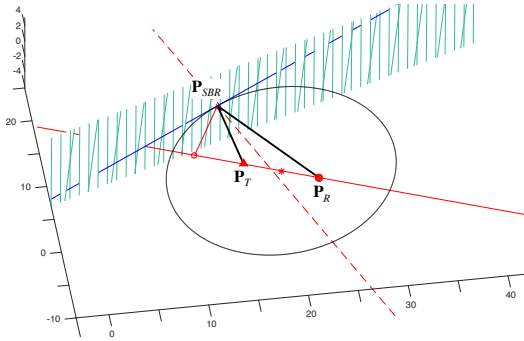


**Fig. 3:** A reflection plane is tangent to the SBR ellipse  $(P_T, P_R, \ell)$ , and is perpendicular to the path plane  $(P_T, P_R, P_{SBR})$ .

is unique for each SBR point. The parametric equation of an ellipse in 3D space is given by

$$\mathbf{x}(t) = c + a \cos(t)\mathbf{u} + b \sin(t)\mathbf{v}, \quad (2)$$

where  $a$  is the major semiaxes,  $b$  is the minor semiaxes,  $c$  is the half distance between foci (linear eccentricity), and  $\mathbf{u}, \mathbf{v}$  are unit vectors for major and minor semiaxis. We find the parameter  $t$  for a reflection point on the ellipse by solving (2). A normal vector to the ellipse at point  $\mathbf{x}(t)$  is given by

$$\mathbf{n}(t) = b \cos(t)\mathbf{u} + a \sin(t)\mathbf{v} \quad (3)$$

This vector is on the path plane, and is normal to the reflector plane. Then, reflector planes, given by reflection points and normal vectors, are parameterized in  $(\theta, \phi, \rho)$  domain. This is a continuous Hough transformation of the SBR points.

A 2D hough image is produced by slicing the 3D hough space in a direction of interest. In order to extract vertical walls, all the points in Hough space with  $\phi = \pi/2 \pm \pi/10$  are selected and added to a 2D hough accumulator after discretization. The accumulator is a 2D grid in polar coordinates, which can be seen as an intensity image. It is created by producing a weighted 2D histogram with weights equal to path powers. This 2D image is then processed to extract features that correspond to the building walls. The intensity peaks in the Hough image correspond to the common tangents to ellipses, i.e., large reflector planes. First, a low-pass filter is applied to the image for noise reduction and enhancing large scale structures. This filter has a truncated circular Gaussian kernel with standard deviation  $\sigma_g$ , which is tuned empirically. The filter is truncated at  $3\sigma_g$ . Detection is done by adaptive thresholding. The threshold value is the local noise level plus the average intensity of the image. A moving average filter of size  $6\sigma_g$  calculates a local noise level for every pixel. The next step is finding a weighted center of mass for each peak region in the binary image. The weights are the intensity values in the original Hough image. These centroids are extracted as reflector planes. The original Hough image is masked with the detected binary image, then transformed to the Cartesian coordinates. Each peak region in the Cartesian coordinates is filtered separately using a 2D linear kernel, i.e., a moving average, in the direction of the corresponding centroid. This enhances the structures that align with the extracted reflector planes, and produces the final map.

## 4. EMPIRICAL RESULTS

The real-world measurement data was obtained by a measurement campaign performed in Aalto University (former TKK) using a 5.3 GHz channel sounder in WILATI project [4]. The measurement signal had a bandwidth of 120 MHz with transmission power of 0.5 watts. Tx and Rx had 32 element semi-spherical and cylindrical antenna arrays respectively. The measurements are performed in an open space inside a modern three-story building with diverse construction materials and large objects in the interior area. The receiver had a fixed known position. The transmitter was moved on a trolley through several routes inside the building while performing measurements. Fig. 4 shows the floor plan of the building and the measurement routes. These routes are approximate, since the exact position and orientation of the Tx at each measurement point is not available. Fig. 5 shows the estimated coordinates of for 400 snapshots in route 2, before and after smoothing. These are the parameters of detected LOS paths transferred to Cartesian coordinates. The resulting Tx locations are presented in Fig. 4 on top of the reference routes. The estimated Tx trajectories have a good match with the planned routes. Note that, the reference routes are not exactly followed during the measurement, hence the ground truth for Tx positions is not available.

Fig. 6 shows the result for detection of SBR points and the detection of vertical plane reflectors using Hough detector. The 2D Hough image in Fig. 6b is a slice of Hough space with near-vertical planes, i.e.,  $\phi = \pi/2 \pm \pi/10$ . Detected peak regions in this image are transformed to Cartesian coordinates and shown in Fig. 6c. The lines in this figure are the centroids of the detected peak regions in Fig. 6b. They correspond to the walls or other planar reflectors. The final scatter map corresponding to vertical reflecting planes, i.e., walls, is shown in Fig. 7. Some of the inner walls are clearly visible in the

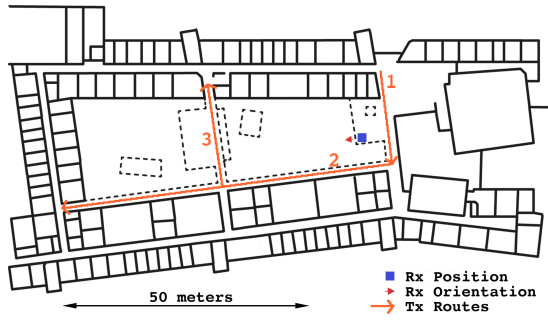


Fig. 4: Floor plan, Rx position, planned Tx routes, and the estimated Tx trajectories. The measurements are done in a lobby area in the 2nd floor. There is LOS visibility between Rx and Tx. The figure shows the estimated Tx trajectories (dashed blue lines) that have a good match with the reference routes.

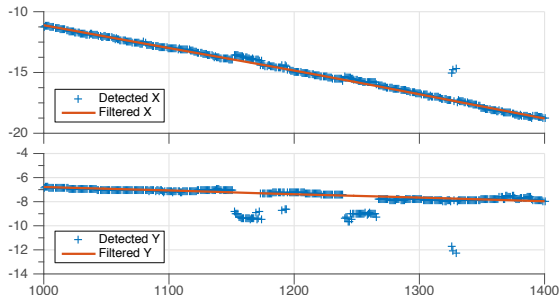
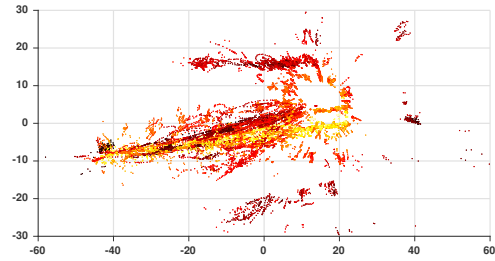


Fig. 5: Parameters of LOS paths for measurement route 2 in Cartesian coordinates. Filtration eliminates errors and outliers.

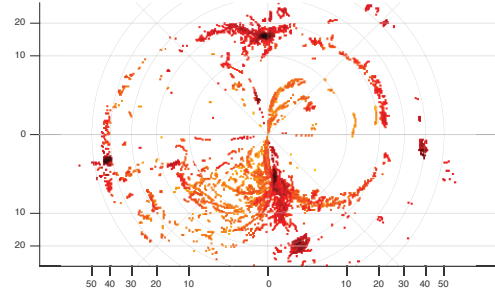
image and they have a good match with the floor plan. The best results are obtained for a long wall parallel to the Tx route 2. A line fitted to this wall, seen in Fig. 6c, has a distance error of 36 cm from the origin and an orientation error of 1.5 degrees with respect to the actual wall. The fixed position of the Rx limited the coverage of the produced map, e.g., there is no SBR path coming from the upper right region in Fig. 7. A complete map may be produced by performing measurements at multiple Rx positions. Two reflectors are detected outside the building, which could be delayed images of the outer walls. Excess delays due to propagation through the walls are not compensated for in our model. The results demonstrate that with advanced processing it is possible to detect long segments of the walls and build a map of an indoor environment using microwave-frequency MIMO measurements. Earlier results using a similar radio bandwidth had a lower precision (higher variability), and were not able to detect the extents of the walls. There is no commonly used method in the literature for numerical analysis of indoor imaging solutions. Moreover, results obtained in different environments are not thoroughly comparable. Given these considerations, our results are comparable to UWB SAR images, which require a higher bandwidth and a complex hardware and measurement scenario [5].

## 5. CONCLUSIONS

There is a growing interest in indoor mapping using radio-frequency or acoustic measurements. In this paper, a novel technique was proposed for producing indoor maps using MIMO radio channel measurements. A ray-tracing method was developed to detect SBR paths and reflection points. The Hough detector method was proposed



(a) Scatter map of SBR points, top view.



(b) Hough transform of the SBR points.



(c) Detected reflector planes

Fig. 6: Detected SBR points are transferred to Hough space. The 2D Hough image (b) is a slice of the Hough space for near-vertical planes. The image is in polar coordinates  $(\rho, \theta)$ ; The filtration and peak detection in Hough image results in several clusters (c) corresponding to strong planar reflectors.

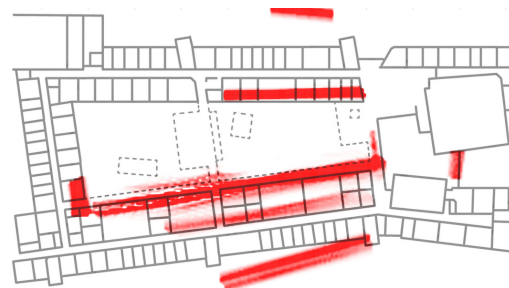


Fig. 7: Final scatter map corresponding to vertical reflecting planes. The measurements did not cover most of the left side.

for extracting planar structures from the cloud of reflection points. The results obtained using real-world measured data demonstrated that the algorithm is capable of producing a map of the walls in a complex indoor environment. Such results have not been reported in previous experiments other than UWB measurements. This provides an opportunity for indoor mapping using MIMO wireless devices and future mobile phones. Future work will focus on higher-order reflections, and model non-planar objects, e.g., pillars and corners.

## 6. REFERENCES

- [1] Hassan Naseri and Visa Koivunen, "Indoor mapping based on time delay estimation in wireless networks," *IEEE Int'l Conference on Acoustics, Speech and Signal Processing (ICASSP 2015)*, 2015.
- [2] Andreas Richter, *Estimation of radio channel parameters: Models and algorithms*, Ph.D. thesis, TU Ilmenau, 2005.
- [3] Jussi Salmi, *Contributions to measurement-based dynamic MIMO channel modeling and propagation parameter estimation*, Ph.D. thesis, Aalto University, 2009.
- [4] Veli-Matti Kolmonen, Peter Almers, et al., "A dynamic dual-link wideband MIMO channel sounder for 5.3 GHz," *IEEE Trans. on Instrumentation and Measurement*, vol. 59, no. 4, 2010.
- [5] Calvin Le, Traian Dogaru, et al., "Ultrawideband (UWB) radar imaging of building interior: measurements and predictions," *IEEE Trans. on Geoscience and Remote Sensing*, vol. 47, no. 5, pp. 1409–1420, 2009.
- [6] Traian Dogaru, DaHan Liao, and Calvin Le, "Three-dimensional radar imaging of buildings based on computer models," in *SPIE Defense, Security, and Sensing*. International Society for Optics and Photonics, 2013, pp. 87140L–87140L.
- [7] Eva Lagunas, Moeness G Amin, et al., "Determining building interior structures using compressive sensing," *Journal of Electronic Imaging*, vol. 22, no. 2, pp. 021003–021003, 2013.
- [8] Xue Yao, Guolong Cui, et al., "Building layout imaging with spatial filtering based on image optimization," in *2014 IEEE Radar Conf. IEEE*, 2014, pp. 1094–1097.
- [9] David Insana and Carey M Rappaport, "Using FDFD technique in two-dimensional te analysis for modeling clutter in wall penetrating radar," *International Journal of Antennas and Propagation*, vol. 2014, 2014.
- [10] Yong Jia, Guolong Cui, et al., "Multichannel and multiview imaging approach to building layout determination of through-wall radar," *IEEE Geoscience and Remote Sensing Letters*, vol. 11, no. 5, pp. 970–974, 2014.
- [11] Bo Chen, Tian Jin, et al., "Building interior layout reconstruction from through-the-wall radar image using MST-based method," *EURASIP Journal on Advances in Signal Processing*, vol. 2014, no. 1, pp. 1–9, 2014.
- [12] Heinrich Luecken and Armin Wittneben, "UWB radar imaging based multipath delay prediction for NLOS position estimation," in *IEEE Int'l Conf. on Ultra-Wideband (ICUWB 2011)*. IEEE, 2011, pp. 101–105.
- [13] Pawan Setlur, Moeness Amin, and Farhan Ahmad, "Multipath model and exploitation in through-the-wall and urban radar sensing," *IEEE Trans. on Geoscience and Remote Sensing*, vol. 49, no. 10, pp. 4021–4034, 2011.
- [14] Michael Leigsnering, Moeness Amin, et al., "Multipath exploitation and suppression for SAR imaging of building interiors: An overview of recent advances," *IEEE Signal Processing Magazine*, vol. 31, no. 4, pp. 110–119, 2014.
- [15] Vincenzo La Tosa, Benoît Denis, and Bernard Uguen, "Joint anchor-less tracking and room dimensions estimation through IR-UWB peer-to-peer communications," in *IEEE Int'l Conf. on Ultra-Wideband (ICUWB 2011)*. IEEE, 2011, pp. 575–579.
- [16] M Des Noes and B Denis, "Benefits from cooperation in simultaneous anchor-less tracking and room mapping based on impulse radio-ultra wideband devices," in *19th Int'l Conf. on Systems, Signals and Image Processing (IWSSIP 2012)*. IEEE, 2012.
- [17] Jianguang Liu, Guolong Cui, et al., "Sidewall detection using multipath in through-wall radar moving target tracking," *IEEE Geoscience and Remote Sensing Letters*, vol. 12, no. 6, 2015.
- [18] Fabio Antonacci, Jason Filos, et al., "Inference of room geometry from acoustic impulse responses," *IEEE Trans. on Audio, Speech, and Language Processing*, vol. 20, no. 10, 2012.
- [19] Ivan Dokmanić, Reza Parhizkar, et al., "Acoustic echoes reveal room shape," *Proceedings of the National Academy of Sciences*, vol. 110, no. 30, 2013.
- [20] Ivan Dokmanic, Reza Parhizkar, et al., "Euclidean distance matrices: Essential theory, algorithms, and applications," *IEEE Signal Processing Magazine*, vol. 32, no. 6, pp. 12–30, 2015.
- [21] Tobias Deissler and Jörn Thielecke, "UWB SLAM with Rao-Blackwellized Monte Carlo data association," in *Int'l Conf. on Indoor Positioning and Indoor Navigation (IPIN)*. IEEE, 2010.
- [22] Erik Leitingner, Paul Meissner, et al., "Simultaneous localization and mapping using multipath channel information," in *IEEE International Conf. on Communication Workshop (ICCW 2015)*. IEEE, 2015, pp. 754–760.
- [23] Michael Leigsnering, Fauzia Ahmad, et al., "Multipath exploitation in sparse scene recovery using sensing-through-wall distributed radar sensor configurations," in *IEEE International Conf. on Acoustics, Speech and Signal Processing (ICASSP 2015)*. IEEE, 2015.
- [24] Hassan Naseri and Visa Koivunen, "Cooperative simultaneous localization and mapping by exploiting multipath propagation," *submitted to IEEE Transactions on Signal Processing*, 2016.
- [25] Robert Ghrist, H Owen, and Michael Robinson, "DTIME: Discrete topological imaging for multipath environments," 2010.
- [26] Juho Poutanen, Katsuyuki Haneda, et al., "Development of measurement-based ray tracer for multi-link double directional propagation parameters," in *3rd European Conf. on Antennas and Propagation (EuCAP 2009)*. IEEE, 2009.
- [27] Juho Poutanen, Katsuyuki Haneda, et al., "Analysis of radio wave scattering processes for indoor MIMO channel models," in *IEEE 20th Int'l Symposium on Personal, Indoor and Mobile Radio Communications*. IEEE, 2009, pp. 102–106.
- [28] Panawit Hanpinitasak, Kentaro Saito, et al., "Clustering method based on scatterer locations for indoor dynamic MIMO channel," in *10th European Conf. on Antennas and Propagation (EuCAP)*. IEEE, 2016, pp. 1–4.
- [29] Richard O Duda and Peter E Hart, "Use of the Hough transformation to detect lines and curves in pictures," *Communications of the ACM*, vol. 15, no. 1, pp. 11–15, 1972.
- [30] Dave Laurenson and Peter Grant, "A review of radio channel sounding techniques," in *Proc. EUSIPCO*, 2006.
- [31] Jussi Salmi, Andreas Richter, and Visa Koivunen, "Detection and tracking of MIMO propagation path parameters using state-space approach," *IEEE Trans. on Signal Processing*, vol. 57, no. 4, pp. 1538–1550, 2009.
- [32] The MathWorks, Inc., *Curve fitting toolbox: user's guide*, The MathWorks, Inc., March 2016.
- [33] Hassan Naseri, J. Salmi, and V. Koivunen, "Synchronization and ranging by scheduled broadcasting," *IEEE Int'l Conference on Acoustics, Speech and Signal Processing (ICASSP 2013)*, 2013.